

# Self-Diffusion Measurements in Methane by Pulsed Nuclear Magnetic Resonance

RAPIER DAWSON, FOUAD KHOURY, and RIKI KOBAYASHI

Rice University, Houston, Texas

The self-diffusion coefficient of methane has been measured from 150° to 350°K. and from 200 to 5,000 lb./sq. in. abs. At constant temperature, the density-diffusivity product is constant up to neighborhood of critical density and decreases sharply above that density. The temperature dependence of the low density data agrees with Chapman-Enskog theory. The Lennard-Jones (6-12) parameters determined from the low density data ( $\epsilon/k = 130^\circ\text{K}$ ,  $\sigma = 3.85\text{\AA}$ .) are in good agreement with those determined by other methods. A correlation for the self-diffusion coefficient for methane has been developed which may provide predictions of other spherical nonpolar gases.

The coefficient of self-diffusion was considered (9) to be the limiting case of the binary diffusion coefficient until Carr and Purcell (2) developed the pulsed (or spin echo) nuclear magnetic resonance (NMR) technique to measure self-diffusion. Directly, the study of this significant transport property, self-diffusion, has led to interesting results.

The self-diffusion coefficient has considerable theoretical interest. It is the transport coefficient most easily calculated by kinetic theory, and it provides a good check for the various theories of the dense gas state. The possibility exists (1) that binary (mutual) diffusion coefficients may be calculated from the self-diffusion coefficients of the two pure components. The measurement of the self-diffusion coefficient of methane in the dilute and dense gas regions is reported here.

## THEORY

### Theory of Self-Diffusion

The molecules in a fluid are continuously in motion. In a uniform homogeneous fluid, this motion is random and represents the thermal energy present in all fluids. This random motion causes any particular molecule of the fluid to move from place to place in the fluid; this movement is called *self-diffusion*.

The coefficient of self-diffusion is defined as

$$D = \langle r^2 \rangle / (6t) \quad (1)$$

where  $\langle r^2 \rangle$  is the mean square net distance a molecule moves in time  $t$ . This definition is consistent with the Ficks law definition of a binary diffusion coefficient,  $D_{12}$ :

$$\frac{\partial C}{\partial t} = D_{12} \nabla^2 C \quad (2)$$

On this basis  $D$  is defined as the limit of  $D_{12}$  as the molecules of 1 and 2 become identical.

In the past, the closest approach to the limit of identical molecules was obtained by observing diffusion of isotopes. For example,  $\text{C}^{14}$  methane may be observed diffusing in  $\text{C}^{12}$  methane (20). The radioactivity of the former and the nuclear stability of the latter serves to distinguish the two and allows the motion of particular methane molecules to be observed. The change in the diffusion coefficient, caused by the difference in molecular weight of the two species, is small but not negligible. Spin echo NMR fol-

lows the molecules by observing their nuclear spin states; this is a much more subtle "tag."

### Spin Echo NMR

The basic method of generating nuclear spin echos was discovered by Hahn (7), who also suggested their use for measuring self-diffusion coefficients. His suggestions were clarified and the experimental methods improved by Carr and Purcell (2).

The self-diffusion coefficient is measured through its effect on the amplitude of a spin echo. This amplitude is given by the equation

$$A = A_0 \exp \left( -\frac{t}{T_2} - \frac{\gamma^2 G^2 D t^3}{12} \right) \quad (3)$$

NMR is usually done in a large uniform magnetic field; the equation above is derived for the case of a small linear field gradient superimposed on the constant field. Measurement of  $D$  by using this equation is straightforward; the technique used in these studies has been described by Douglass and McCall (4).

## APPARATUS

The spectrometer used in this work was a model PS-1 made by NMR Specialties. It has a 60 MHz coherent pulse unit which produced 50 to 100 w. of pulsed RF power. A single coil sample circuit was used.

The magnet used was a superconducting solenoid made by Westinghouse. The solenoid was designed to have high magnetic field uniformity up to its maximum field of 25 kilogauss. The magnet wire was 75% niobium-25% zirconium. The Dewar used provided a 1.75 in. diameter room temperature access hole into the magnetic field.

No automatic locking device to couple the magnetic field and the spectrometer frequency was used. Both the superconductor and the crystal oscillator in the spectrometer were quite stable without appreciable drift.

The magnetic field gradient was applied with a pair of opposed Helmholtz coils wound outside the solenoid and Dewar. A constant current supply energized the coils. Since both the magnet and the Dewar were completely nonferromagnetic, the applied gradient was not distorted to any extent. The applied gradient was calibrated by use of a flux-gate magnetometer.

The temperature of the sample was controlled by circulating liquid from a constant temperature bath through a jacket around the sample bomb. The temperature was measured with calibrated thermocouples at each end of the bomb. Although the bomb was in a Dewar flask, there were temperature gradients along the length of the bomb. These gradients were not more than 0.5°K.

The sample being measured was contained in the NMR sam-

Rapier Dawson is with Esso Production Research Company, Houston, Texas.

TABLE 1. EXPERIMENTAL VALUES OF THE DIFFUSIVITY

$T = 353.8^{\circ}\text{K.}$			$T = 322.5^{\circ}\text{K.}$			$T = 297.0^{\circ}\text{K.}$			
$P$ , lb./sq.in.abs	$\rho$ , g./cc.	$\rho D \times 10^6$ , g./ (cm.)(sec.)	$P$ , lb./ sq.in.abs.	$\rho$ , g./cc.	$\rho D \times 10^6$ , g./ (cm.)(sec.)	$P$ , lb./ sq.in.abs.	$\rho$ , g./cc.	$\rho D \times 10^6$ , g./ (cm.)(sec.)	$P$ , lb./ sq.in.abs.
993	0.03933	167.4	709	0.03106	155.5	771	0.03793	145.6	322
1,256	0.05025	166.6	945	0.04216	154.5	982	0.04944	146.0	451
1,680	0.06803	162.3	1,185	0.05375	154.7	1,386	0.07281	149.5	598
2,138	0.08713	164.8	1,489	0.06876	157.0	1,846	0.1003	148.0	731
2,640	0.10737	165.0	1,851	0.08682	156.7	2,370	0.13076	147.0	928
3,498	0.13912	162.4	2,264	0.10712	155.2	3,020	0.16405	144.5	1,115
4,699	0.17614	154.3	2,975	0.13965	153.1	4,161	0.2083	137.0	1,447
6,025	0.2079	150.0				5,996	0.2539	127.4	1,816
									2,270
									3,100
									4,350
									5,935
$T = 197.7^{\circ}\text{K.}$			$T = 190.9^{\circ}\text{K.}$			$T = 187.1^{\circ}\text{K.}$			
112	0.00801	105.4	230	0.01833	102.6	251	0.02097	98.3	199
198	0.01480	105.1	280	0.02318	98.6	349	0.03182	98.2	241
303	0.02406	102.7	335	0.02892	98.4	448	0.04611	103.6	299
419	0.03618	103.9	390	0.03542	99.0	536	0.0655	103.6	341
555	0.05499	105.7	455	0.04448	102.4	1,380	0.3017	82.5	368
644	0.07263	107.2	532	0.05808	105.9	4,530	0.3584	65.6	407
1,101	0.2485	99.2	595	0.07422	105.2				1,464
1,991	0.2967	88.4	625	0.08578	107.6				3,958
			857	0.2580	90.0				
			3,950	0.3463	71.1				

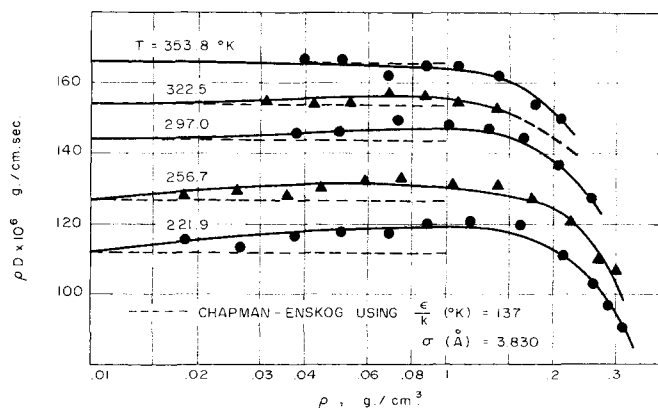
ple coil, which was inside the high pressure bomb. The bomb was made of beryllium-copper and was tested at 7,000 lb./sq.in. The pressure was measured with calibrated Heise gauges in the appropriate pressure range. The sample gas was ultra high purity methane, used as supplied.

#### DISCUSSION OF THE EXPERIMENTAL ERRORS

The NMR measurements gave the self-diffusion coefficient of the sample in a direct fashion. The two sources of error gave a total uncertainty of  $\pm 6\%$  in each data point. Half of this error is systematic error associated with the value of the magnetic field gradient. The other errors are random and may be seen in the graphs of the data. The random errors had many sources, including the temperature and pressure measurements and small changes in the NMR apparatus.

Although temperature and pressure do not enter into the measurements of the self-diffusion coefficient, they must be known accurately to define the system being measured.

$T = 256.7^{\circ}\text{K.}$			$T = 221.9^{\circ}\text{K.}$		
$\rho$ , g./cc.	$\rho D \times 10^6$ , g./ (cm.)(sec.)	$P$ , lb./ sq.in.abs.	$\rho$ , g./cc.	$\rho D \times 10^6$ , g./ (cm.)(sec.)	
0.01844	128.0	279	0.01848	115.9	
0.02571	129.5	384	0.02651	113.9	
0.03524	128.1	511	0.03726	116.7	
0.04451	130.9	646	0.05043	117.9	
0.05929	132.1	803	0.06872	117.9	
0.07461	133.0	941	0.08827	120.2	
0.10416	131.7	1,108	0.11698	121.0	
0.13788	131.2	1,304	0.16121	119.9	
0.1744	127.6	1,720	0.2129	111.5	
0.2210	120.4	2,407	0.2572	103.5	
0.2622	109.9	3,398	0.2896	97.2	
0.2939	106.2	4,557	0.3131	90.4	
$T = 173.4^{\circ}\text{K.}$			$T = 154.5^{\circ}\text{K.}$		
0.01797	87.6	141	0.014286	82.3	
0.02265	86.5	175	0.018704	79.9	
0.03041	88.6	216	0.3511	58.1	
0.03717	89.5	3,460	0.3894	46.5	
0.04244	90.1				
0.3021	75.7				
0.3355	65.8				
0.3704	57.8				

Fig. 1.  $\rho D$  vs.  $\rho$  for several supercritical isotherms.

Self-diffusion is best expressed as a function of temperature and density. Temperature was measured to  $\pm 0.2^{\circ}\text{K.}$  and the pressure to  $\pm 0.2\%$ . The density was calculated from an equation of state developed by Venn (19). In general, the error in density was  $\pm 0.1\%$ , somewhat less than the error in the self-diffusion coefficient. However, close to the critical point the density calculation became much more difficult and our results became less accurate; therefore, results in the direct vicinity of the critical region are not presented.

## RESULTS

The results at various temperatures are shown in Figure 1 and tabulated in Table 1. The data are shown as plots of the density-diffusivity product  $\rho D$  vs. density. This type of plot best reveals the density dependence of the self-diffusion coefficient.

The most noticeable feature of the data is that  $\rho D$  is almost constant up to the critical density; then  $\rho D$  begins to decrease sharply as densities typical of fluids are reached. This type of behavior has been observed (8, 10) in other gases.

The data may be cross plotted to show the temperature dependence of the diffusion coefficient at constant density. Figure 2 shows such a cross plot made at  $\rho = 0.02$  g./cc.

Temperature dependent data at dilute gas densities may be used to determine Lennard-Jones (6-12) parameters by use of Chapman-Enskog (9) theory. The first-order Chapman-Enskog theory gives the self-diffusion coefficient as

$$D = 0.002628 \frac{\sqrt{T^3/M}}{P\sigma^2 \Omega^{(1,1)*}} \quad (4)$$

Use of the ideal gas law  $P = \rho RT/M$  reduces this to

$$\rho D = 32.03 \times 10^{-6} \frac{\sqrt{TM}}{\sigma^2 \Omega^{(1,1)*}} \quad (5)$$

This equation is used to determine which values of the parameters  $\sigma$  and  $\epsilon/k$  give the best fit of the data over a range of temperatures. The parameters determined from the temperature dependence at  $\rho = 0.02$  g./cc. are  $\epsilon/k = 130^\circ\text{K.}$  and  $\sigma = 3.85\text{\AA.}$  These parameters fit the 0.02 g./cc. isochore with an average error of 1%. Figure 2 compares the calculated and experimental (3) values of  $\rho D$ .

Table 2 shows a comparison of Lennard-Jones parameters determined by various methods. The agreement of the parameters determined from self-diffusion with those from other methods is good. The agreement supports the use of Chapman-Enskog theory to predict self-diffusion coefficient and contrasts with some preliminary data (13) which indicated that errors would result. Note that the determination of Lennard-Jones parameters from temperature dependence is not highly sensitive. For example, the parameters  $\epsilon/k = 148^\circ\text{K.}$ ,  $\sigma = 3.76\text{\AA.}$  fit the  $\rho = 0.02$  g./cc. data

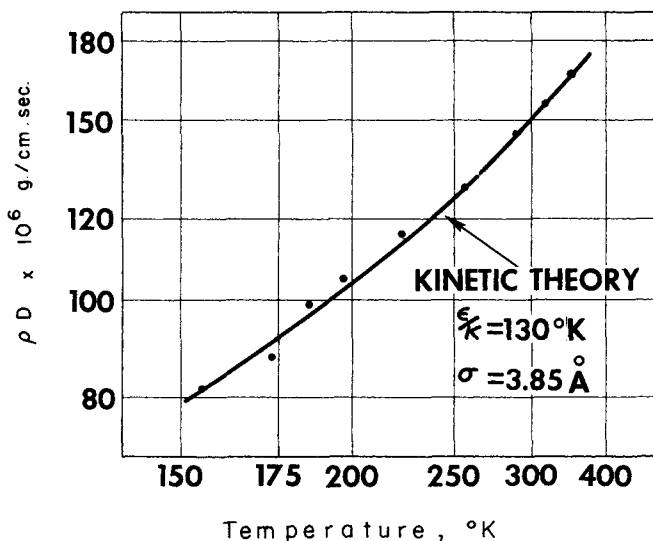


Fig. 2. Comparison of experimental low density results with values predicted by kinetic theory for methane at  $\rho = 0.02$  g./cc.

of this work with an average deviation of 1.3% from the experimental data as compared with the 1% deviation using  $\epsilon/k = 130^\circ\text{K.}$  and  $\sigma = 3.85\text{\AA.}$

The temperature dependence shown in Figure 2 at  $\rho = 0.02$  g./cc. is closely fit by an Arrhenius relation to give the activation energy for diffusion of about 0.4 kcal./mole.

## CORRESPONDING STATES CORRELATION

The similarity of the shapes of the  $\rho D$  isotherms (Figure 1) suggests that those isotherms may be collapsed into a single line by factoring out the temperature dependence. Thus, Figure 3 shows a plot of all the data plotted as  $\rho D/(\rho D)_0$  vs. density where  $(\rho D)_0$  is the low density value of the density-diffusivity product. In Figure 3,  $(\rho D)_0$  is calculated from Chapman-Enskog theory [that is, Equation (5)], although an experimental value could also be used.

The temperature independence of  $\rho D/(\rho D)_0$  may be interpreted on a theoretical basis if the self-diffusion equation given by Douglass et al. (5) for high densities is used. This equation, based on a rigid sphere model, may be written as

$$\rho D \propto (T)^{1/2} \rho \left[ \frac{(PV)}{(RT)} - 1 \right]^{-1} \quad (6)$$

and from the simplified kinetic theory of dilute gases (9)

$$\rho D \propto (T)^{1/2} \quad (7)$$

The reduced value  $\rho D/(\rho D)_0$  will be

$$\frac{\rho D}{(\rho D)_0} = k\rho \left[ \frac{(PV)}{(RT)} - 1 \right]^{-1} \quad (8)$$

The use of the volume virial expansion for  $(PV)/(RT)$  gives

$$\begin{aligned} \frac{\rho D}{(\rho D)_0} &= k\rho \left[ 1 + \frac{B}{V} + \frac{C}{V^2} + \dots - 1 \right]^{-1} \\ &= k\rho [B\rho + C\rho^2 + \dots]^{-1} \end{aligned} \quad (9)$$

The virial coefficients  $B, C, \dots$  are temperature independent for rigid spheres. Division of the polynomial results

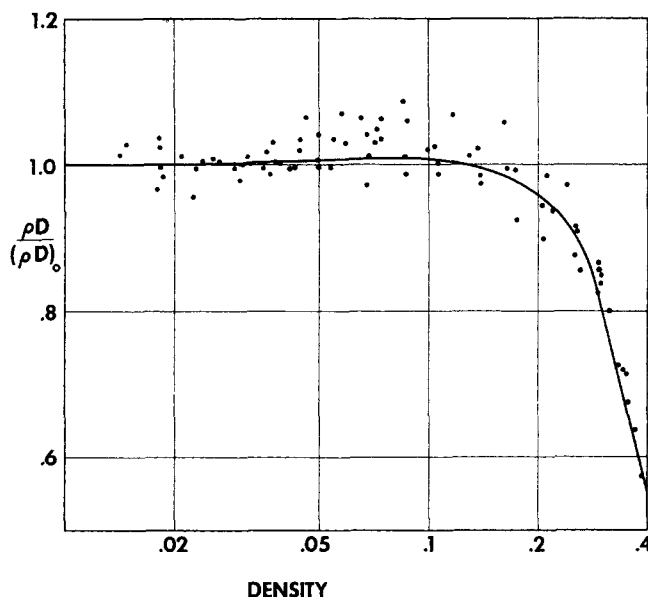


Fig. 3. Methane self-diffusion data between  $154^\circ$  and  $354^\circ\text{K.}$ , reduced by dividing by the kinetic theory value of  $\rho D$  at the various temperatures.

TABLE 2.

Method	$\epsilon/k$ (°K.)	$\sigma$ (Å.)	Ref.
Self-diffusion	130	3.85	This work
Self-diffusion	148	3.82	(18)
Viscosity	137	3.822	(9)
Viscosity	144	3.796	(9)
Second virial	148	3.817	(9)
Crystal structure	148	4.22	(11)

in

$$= k\rho \left[ \frac{b'}{\rho} + c' + d'\rho + e'\rho^2 + \dots \right]$$

$$= k [b' + c'\rho + d'\rho^2 + \dots] \quad (10)$$

As the density is reduced,  $(\rho D)$  approaches  $(\rho D)_0$ ; that is, as  $\rho \rightarrow 0$ ,  $(\rho D)/(\rho D)_0 \rightarrow 1$ ,  $(kb') \rightarrow 1$ , and

$$\frac{\rho D}{(\rho D)_0} = 1 + b\rho + c\rho^2 + d\rho^3 + \dots \quad (11)$$

A calculation of the coefficients for Equation (11) was made by using the least-squares method and by stopping at the fourth term of the polynomial with the eighty-three experimental data presented in Table 1. The values of  $\epsilon/k$  and  $\sigma$  from this work were used. The average error for this calculation was 2.2%.

During the course of review of this paper, the authors were able to obtain additional NMR methane self-diffusion data by Oosting (16). Eighty-seven saturation and isochoric data from 90° to 308°K. and up to a reduced density of 1.04 were combined with our data to determine the same coefficients. The average error was 2.06%. This excellent agreement of the two independent data sets led to a third calculation which added sixty-two isothermal data by Oosting at 194.8°, 273.15°, and 298.15°K. up to a density of 575 amagat (reduced density of 2.55). The average error for this calculation was 2.34% by using eighty-three data of this work and 149 data of Oosting. The three coefficients are

$$\begin{aligned} b &= 0.329826 \\ c &= -1.15006 \\ d &= -6.99167 \end{aligned}$$

The calculated curve, as well as the experimental points of this work, are shown in Figure 3.

Written in terms of the reduced density, Equation (11) becomes

$$\frac{\rho D}{(\rho D)_0} = 1 + b_r \rho_r + c_r \rho_r^2 + d_r \rho_r^3 \quad (12)$$

By using  $\rho_c = 0.162$  g./cc.

$$\begin{aligned} b_r &= 0.053432 \\ c_r &= -0.030182 \\ d_r &= -0.029725 \end{aligned}$$

This line, shown in Figure 4, correlates the density dependence of  $(\rho D)$  for a reduced density from 0.05 to 2.55. This correlation is based on data between reduced temperatures of 0.48 and 1.8 and should be useful over a wider range than this.

We have compared this correlation with various published self-diffusion data. In these comparisons, the  $(\rho D)_0$  value was taken from the data in question. Below the critical density, self-diffusion has been measured in several gases. These authors (6, 10, 12, 15) all concluded that  $\rho D$  is constant below the critical density; their data agree

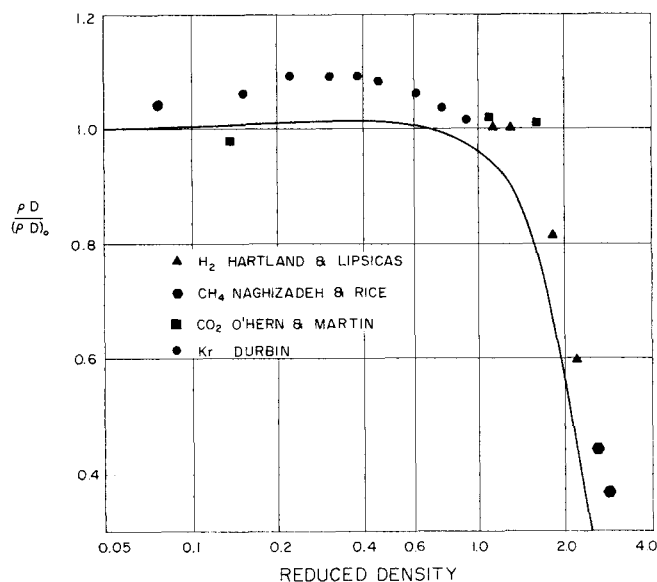


Fig. 4. Correlation of the density dependence of  $\rho D$ . Some other results are shown for comparison.

well with the present correlation and are not shown. Hartland and Lipsicas (8) observed the self-diffusion of hydrogen at 36° and 55°K. up to about twice the critical density. Points representing these data using their low density limit are shown in Figure 4; the agreement appears good. The smoothed data of Durbin (6) are given for his entire density range at 308°K. The choice of the limiting low density value is important in the evaluation of the data. The data on carbon dioxide (15) for three temperatures, 273°, 308°, and 373°K., are also shown. In addition, Figure 4 shows some of the liquid methane data of Naghizadeh and Rice (14). The latter data were reduced by using values of  $(\rho D)_0$  obtained by the same Chapman-Enskog theory calculation used with the present data.

The present correlation may also be compared with the theoretical correlation developed by Slattery and Bird (17) using modified Enskog theory. Here the agreement is only qualitative (average error  $\approx 10\%$ ). When plotted as  $\rho D$  vs. density (3), the Bird-Slattery correlation shows the sharp drop above the critical density and predicts (well above the critical temperature) a constant value of  $\rho D$  below the critical density. However, the  $\rho D$  curves also show unusual minima and maxima which are probably unrealistic.

## CONCLUSIONS

The self-diffusion coefficient has been measured and is reported in the range 154°K.  $< T < 353^\circ\text{K.}$  and 200 lb./sq.in.abs.  $< P < 5,000$  lb./sq.in.abs., with the exclusion of the critical region. The density-diffusivity product  $\rho D$  is constant, at constant temperature, below the critical density and drops sharply as the density increases above the critical value. The shape of the  $\rho D$  vs.  $\rho$  curves is nearly independent of temperature.

The self-diffusion data below the critical density agree well with results of Chapman-Enskog theory (18) provided the experimental value of density is used. The Lennard-Jones parameters calculated from the data agree well with those found by other methods.

A correlation is presented based on these data and the data of Oosting (16) which will predict the self-diffusion coefficient for methane and other essentially spherical nonpolar gases up to two and one-half times the critical

density and over a wide range of temperature. Application of the correlation requires the limiting low pressure value for the desired gas, obtained by measurement or calculation by the Chapman-Enskog theory.

#### ACKNOWLEDGMENT

The authors wish to thank National Science Foundation for the support of this work and Phillips Petroleum Company for generous supply of hydrocarbons.

#### NOTATION

$A$  = echo amplitude  
 $b, c, d$  = coefficients in polynomial  
 $C$  = concentration of component  
 $D$  = self-diffusion coefficient (sq.cm./sec.)  
 $G$  = magnetic field gradient  
 $k$  = constant; Boltzmann's constant  
 $M$  = molecular weight  
 $P$  = pressure  
 $R$  = gas law constant  
 $r$  = mean square net distance a molecule moves in time  $t$   
 $T_2$  = spin-spin relaxation time  
 $t$  = time delay of echo following exciting pulse  
 $\gamma$  = nuclear gyromagnetic ratio  
 $\rho$  = density, (g./cc.)  
 $\epsilon/k, \sigma$  = Lennard-Jones parameters, °K. and Å.  
 $\Omega^{(1,1)*}$  = collision integral, a function of  $kT/\epsilon$

#### Subscripts

$c$  = critical  
 $o$  = low density limit

$r$  = reduced

#### LITERATURE CITED

1. Bearman, R. J., *J. Chem. Phys.*, **32**, 1308 (1960).
2. Carr, H. Y., and E. M. Purcell, *Phys. Rev.*, **94**, 630 (1954).
3. Dawson, R., Ph.D. thesis, Rice Univ., Houston, Tex. (1966). Available from University Microfilm, Ann Arbor, Michigan.
4. Douglass, D. C., and D. W. McCall, *J. Phys. Chem.*, **62**, 1102 (1958).
5. ———, and E. W. Anderson, *J. Chem. Phys.*, **34**, 152 (1961).
6. Durbin, L., and R. Kobayashi, *ibid.*, **37**, 1643 (1962).
7. Hahn, E. L., *Phys. Rev.*, **80**, 580 (1950).
8. Hartland, A., and M. Lipsicas, *ibid.*, **133A**, 665 (1964).
9. Hirschfelder, J. O., C. F. Curtiss, and R. B. Bird, "Molecular Theory of Gases and Liquids," Wiley, New York (1954).
10. Lipsicas, M., *J. Chem. Phys.*, **36**, 1235 (1962).
11. Mason, E. A., and W. E. Rice, *ibid.*, **22**, 843 (1954).
12. Mifflin, T. R., and C. O. Bennett, *ibid.*, **29**, 975 (1958).
13. Mueller, C. R., and R. W. Cahill, *ibid.*, **40**, 651 (1964).
14. Naghizadeh, J., and S. A. Rice, *ibid.*, **36**, 2710 (1962).
15. O'Hern, H. A., and J. J. Martin, *Ind. Eng. Chem.*, **47**, 2081 (1955).
16. Oosting, P. H., Dissertation, Univ. Amsterdam, Netherlands (1968).
17. Slattery, J. C., and R. B. Bird, *AIChE J.*, **4**, 137 (1958).
18. Trappeniers, N. J., and P. H. Oosting, *Phys. Letters*, **23**, 445 (1966).
19. Vennix, A. J., and Riki Kobayashi, *AIChE J.*, **15**, No. 6, 926 (Nov., 1969).
20. Winn, E. B., *Phys. Rev.*, **80**, 1024 (1950).

Manuscript received July 26, 1968; revision received December 23, 1968; paper accepted December 30, 1968.

# Small Surface Waves and Gas Absorption

G. F. DICK, JR., and J. M. MARCHELLO

University of Maryland, College Park, Maryland

Surface renewal models based on wave induced drift currents are proposed to explain gas absorption data in deep tanks. A model assuming plug surface flow was found to best represent the available data for the absorption of carbon dioxide, oxygen, propylene, and helium into water. Velocities obtained by fitting the mass transfer data agree with experimental velocities obtained from dye studies.

Small waves or ripples have been observed to have a pronounced effect on mass transfer across an air-water interface (1, 6). Goren and Mani (4) studied the effect of standing waves of controlled amplitude and frequency on mass transfer through thin, horizontal, liquid layers. They also conducted dye studies of the drift currents produced by the waves. The objective of this investigation was to study drift motions induced by progressive waves and to develop an applicable absorption model.

#### SURFACE RENEWAL MODELS

Absorption in water is described by the general equations of change for species conservation. The velocity components may, in principle, be obtained from wave hydrodynamics. Classical first-order wave theory predicts

smooth closed particle paths which are ellipses for deep water progressive waves (7). When second-order terms are included, closed particle paths are no longer predicted (5), and there is a net drift velocity.

Stokes (8) proposed a simple expression for the second-order mean velocity in the direction of wave propagation for inviscid fluids. More recently, Longuet-Higgins (5) has developed an expression for the wave drift velocity for viscous fluids. Comparisons of the Longuet-Higgins and Stokes theories with experimental data have been inconclusive (9), but it appears that the Stokes expression is most applicable for deep water waves ( $kd > 1$ ), while the Longuet-Higgins solution best describes shallow water transport.

In the development of the surface renewal models, it is assumed that the water flows away from the generator along the surface. The surface drift flow is strong but shallow and is present over less than one fifth of the total

G. F. Dick, Jr., is with Esso Research and Engineering Company, Baytown, Texas.